AIP Journal of Applied Physics

Depth-resolved ballistic imaging in a low-depth-of-field optical Kerr gated imaging system

Yipeng Zheng, Wenjiang Tan, Jinhai Si, YuHu Ren, Shichao Xu, Junyi Tong, and Xun Hou

Citation: Journal of Applied Physics **120**, 093101 (2016); doi: 10.1063/1.4962163
View online: http://dx.doi.org/10.1063/1.4962163
View Table of Contents: http://scitation.aip.org/content/aip/journal/jap/120/9?ver=pdfcov
Published by the AIP Publishing

Depth-resolved ballistic imaging in a low-depth-of-field optical Kerr gated imaging system

Yipeng Zheng (郑益朋),[1] Wenjiang Tan (谭文疆),[1,a)] Jinhai Si (司金海),[1]
YuHu Ren (任玉虎),[1] Shichao Xu (许世超),[1] Junyi Tong (佟俊仪),[2] and Xun Hou (侯洵)[1]
[1]*Key Laboratory for Physical Electronics and Devices of the Ministry of Education and Shaanxi Key Lab of Information Photonic Technique, School of Electronics and Information Engineering, Xi'an Jiaotong University, Xianning-xilu 28, Xi'an 710049, China*
[2]*Departments of Applied Physics, Xi'an University of Technology, Xi'an 710048, China*

(Received 31 May 2016; accepted 22 August 2016; published online 1 September 2016)

We demonstrate depth-resolved imaging in a ballistic imaging system, in which a heterodyned femtosecond optical Kerr gate is introduced to extract useful imaging photons for detecting an object hidden in turbid media and a compound lens is proposed to ensure both the depth-resolved imaging capability and the long working distance. Two objects of about 15-μm widths hidden in a polystyrene-sphere suspension have been successfully imaged with approximately 600-μm depth resolution. Modulation-transfer-function curves with the object in and away from the object plane have also been measured to confirm the depth-resolved imaging capability of the low-depth-of-field (low-DOF) ballistic imaging system. This imaging approach shows potential for application in research of the internal structure of highly scattering fuel spray. *Published by AIP Publishing*. [http://dx.doi.org/10.1063/1.4962163]

INTRODUCTION

The imaging of objects hidden in a turbid medium has long been a challenging and important problem in many industrial, military, and medical applications. When a light beam is introduced into a turbid medium, the transmitted light comprises three components, i.e., ballistic, snake, and diffuse photons. The ballistic photons traverse the shortest path in the incident direction without scattering. The snake photons scatter slightly in the forward direction after traveling over relatively longer paths. The ballistic and snake components retain significant initial properties and information on the structures of the object submerged in the turbid medium. The diffuse photons travel long distances through multiple scattering within the medium and lose most of the image information.[1] Thus, the multiple-scattered diffuse light provides a noise background which deteriorates and, in extreme cases, may destroy any shadow image of structures inside the turbid medium. Alfano and co-workers developed a technique called ballistic imaging to detect objects merged in a turbid medium.[2] This technique usually devises an optical Kerr gate (OKG; a kind of ultrafast optical switch) that extracts the ballistic and snake photons in the leading edge of the transmitted light pulse, while blocks the diffuse photons that lately arrive because of its longer path. In recent years, Linne *et al*. modified the OKG ballistic imaging approach and added a single-shot technology to view the high-speed breakup of the liquid core in the near field of an atomizing spray.[3,4] The applications for dense spray diagnostics redrew attention to the OKG ballistic imaging system.

Recently, a number of efforts have been proposed to improve the OKG imaging quality. Rozé *et al*. discussed the effects of time gate, optical layout, and wavelength on the OKG ballistic imaging.[5] Dartigalongue *et al*. developed a new OKG experimental setup to isolate either the transmitted or the scattered light from an optically thick medium.[6] Tan *et al*. proposed a heterodyned OKG to improve the image sharpness.[7,8] In addition, a collinear, two-color system with high resolution was demonstrated by Purwar *et al*.[9] To increase the resolution limit of the imaging system by increasing its numerical aperture, Mathieu *et al*. proposed the use of a large-aperture switching beam to trigger the OKG.[10] In the studies mentioned above, the transverse imaging information of the object can be only obtained, and the longitudinal imaging information is lost. It is helpful to obtain depth-resolved ballistic imaging (DRBI) for surveying the longitudinal distribution of the voids, drops, and so on in a fuel spray. In practice, one possible way to implement depth-resolved imaging is decreasing the depth of field, which is the distance between the nearest and farthest subjects in the image that appear acceptably sharp.[11] For example, it is feasible to image different layers of a sample along the optical axis using a microscope. If an ordinary microscopy lens is applied to the OKG imaging system, high spatial frequencies of the object will expand seriously in the Kerr media. A transient spatial aperture induced by the gating beam will filter most of the high spatial frequencies, which will cause the degeneration of the transverse spatial resolution of the imaging system. The high spatial frequencies filtered due to the transient spatial aperture can be compensated by means of a heterodyned OKG.[7]

In the present study, we demonstrated DRBI with a long-working-distance micro-imaging system with a low depth of field (DOF). A compound lens composed of two lenses and an object lens (OL) was added to the OKG ballistic imaging system to ensure both the low DOF and the long working distance, and a heterodyned OKG was used to compensate the high spatial frequencies of the imaging. The working distance is 21.5 cm in our experiment, and the depth resolution of our imaging system is less than 600 μm for a 15-μm object.

a)Electronic mail: tanwenjiang@mail.xjtu.edu.cn

Moreover, a comparative investigation of the depth-resolved capability between the DRBI and the conventional 4*f* ballistic imaging systems was performed under the different scattering environments.

EXPERIMENT

A schematic of our DRBI system is shown in Figure 1. A Ti: sapphire laser system (Libra-USP-HE, Coherent, Inc., CA, USA) emitting 50 fs, 3 mJ, 800 nm laser pulses at a repetition rate of 1 kHz was used in our experiment. The laser beam was split into two by using a beam splitter (BS). The reflective part with 700 mW and the transmitted part with 300 mW were used as the pump beam and the probe beam, respectively. The pump beam was filtered using a short-pass filter (SPF). The polarization direction of the pump beam was rotated by 45° using a $\lambda/2$ wave plate for maximizing gating efficiency. A delay line was used to control the time delay between the pump pulse and the probe pulse. The pump beam was focused into the optical Kerr medium (OKM) with a size of 1 mm by lens L0. The carbon disulfide (CS_2) filled in a glass cuvette with a path length of 1 mm was used here as the optical Kerr material. The probe beam was modulated by the object to be imaged. The modulated light in the low-DOF ballistic imaging system was collected by a compound lens, which was composed of a Lens L1 and an objective lens. The lens L1 with a long focal length was used to ensure the sufficiently long working distance, which was placed about 21.5 cm away from the object. The OL with the numerical aperture of 0.55 was used to ensure the sufficiently low DOF actually. The beam passing through the compound lens was focused onto the OKM located at back focal plane of L2 by lens L2. The arrangement of the OKG used in the DRBI system was the same as in References 12 and 13. A quarter-wave plat was used to enhance heterodyned OKG signal, and the biased angle was 7°. Thereafter, the OKG imaging beam was collected by lens L3 and imaged onto a charge-coupled device camera (CCD) (INFINITY3-1 M-NS-TPM, Lumenera Corporation, Ottawa, Canada) in the imaging system. A long-pass filter (LPF) was placed before the camera to decrease the noise generated by the pump pulse scattering in the OKM.

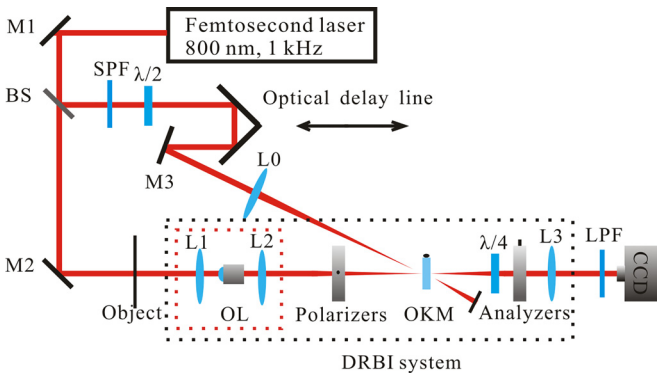

FIG. 1. Depth-resolved ballistic imaging system; SPF: short-pass filter; $\lambda/2$: half-wave plate; $\lambda/4$: quarter-wave plate; BS: beam splitter; OL: objective lens; OKM: optical Kerr material; LPF: long-pass filter; M1, M2, M3: mirrors; L0, L1, L2, and L3: lenses. The part marked with red square frame is the compound lens to ensure both the low DOF and the long working distance.

In what follows, we demonstrate the depth-resolved imaging of an object merged in a turbid medium by using the DRBI system described above. The turbid medium used in our experiment was a suspension of 1.6-μm-diameter polystyrene spheres (PS) with an optical depth (OD) of 5.7 measured by the OKG method.[14] Optical depth is defined as $\mathrm{OD} = -\ln(I/I_0)$, where I is the intensity of the light exiting the scattering medium, and I_0 is the intensity of the light entering the scattering medium. The average power of the probe beam is about 200 mW.

RESULTS AND DISCUSSION

As shown in Figure 2(a), two opaque letters "F" on the surface of two glass slides were used as the imaging object. The lines forming the letters were approximately 15-μm wide. The letters were placed face to face with a small adjustable separation. An inverted "F" was placed in front of an upright "F." As shown in Fig. 2(a), both letters might be clearly imaged to present a pattern "卐" in an imaging system without depth-resolved imaging ability. On the other hand, on

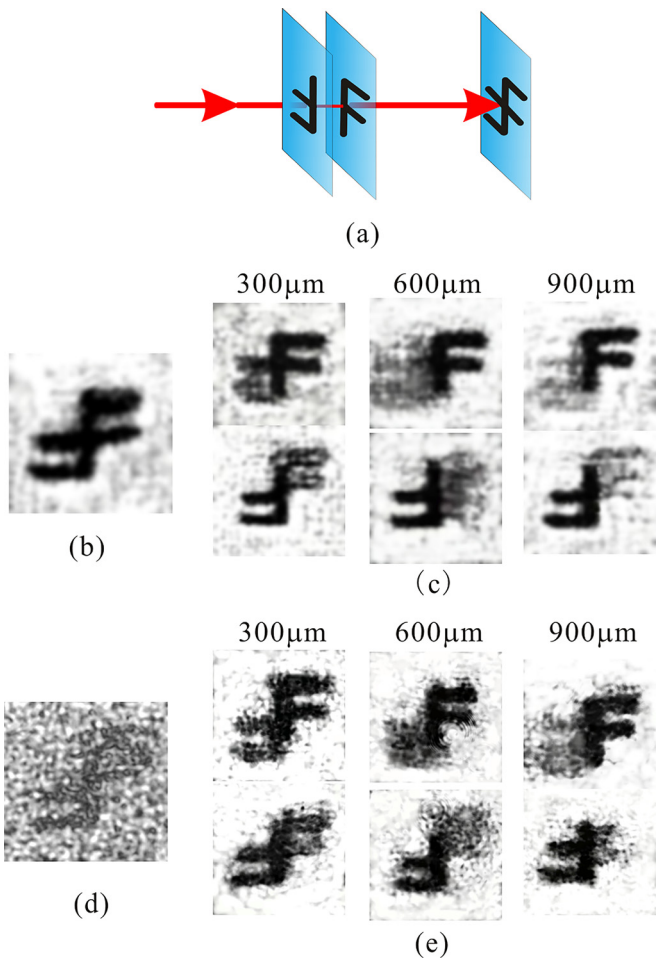

FIG. 2. (a) Sketch of imaging of the letters without depth revolution. (b) Imaging of the letters in water when their separation is 0. (c) Individual imaging of the letters at different separations in water. (d) Direct shadowgraph imaging of panel (e) submerged in a turbid medium. (d) Individual imaging of the letters at different separations in a turbid medium.

using a system with depth-resolved imaging ability, each of the letters might be imaged individually. In our DRBI experiment, a compound lens composed of two lenses and an object lens (OL) was used to ensure both the low DOF and the long working distance. When the CCD was located at the imaging plane of inverted "F," the inverted "F" was imaged explicitly on CCD with the letter "F" blurring and fading. On the contrary, the letter "F" was imaged explicitly.

First, we demonstrate some typical imaging results in our DRBI system. Figure 2(b) shows an image of the letters in water when the separation between the two letters is 0. Both the letters are clearly imaged to present a pattern "". Fig. 2(c) shows the images of the letters in water with different separations. When the separation between the two letters is approximately 300 μm, the image of one letter is disturbed seriously by the shadow of the other one. However, the depth-resolved imaging results of the letters are improved when the separation between the two letters is increased to approximately 600 μm. Furthermore, when the separation is increased to approximately 900 μm, the visualizations of the letters become slightly better due to the shadow fading further. In order to evaluate the depth-resolution of our imaging system, we further compared the depth-resolved imaging quality of letter "F" on the top of Fig. 2(c) by calculating quantitatively the contrast of the invert letter "F," which is a background noise. The contrast of the invert "F" for the separation 300 μm was calculated to be 0.308. When the separation was increased to 600 μm, the contrast decreased to 0.045. The invert "F" is not discernible at this moment. When the separation was further increased to 900 μm, the contrast changed slightly to 0.040 and remains almost unchanged. So, we conclude that the depth-resolution of our imaging system is approximately 600 μm.

Next, we hide the imaging objects in the PS suspension. Figure 2(d) shows a direct image of the object merged in the turbid medium without using the OKG. From Fig. 2(d), we can see that the direct image was blurred owing to the scattered photons that become noise. The imaging of the objects in the turbid medium with the DRBI system is shown in Fig. 2(e). From Fig. 2(e), we can see that the visualization of the objects is improved by using the OKG. The imaging results of the objects in the turbid medium (with scattering) are nearly the same as those of the objects in water. These results indicate that the DRBI system has the capability of about 600-μm depth-resolved imaging for 15-μm-width object in a turbid medium.

It is well-known from geometric optics that only a point in the object plane can sharply focus in the imaging plane. A subject nearer to or farther away from the object plane will form a blurry image with a fixed image distance. Subjects away from the object plane will form blurrier images in a lower-DOF imaging system and, in extreme cases, may merely form a weak background. Therefore, a slice of the object along the object plane might be imaged independently in a low-DOF imaging system, when the subjects far away from the object plane form an acceptable blurred background. Previous research has shown that the width of the near field of a spray cone can reach to several millimeters. The DRBI system demonstrated above could image the near field of the spray with approximately 600-μm depth-revolution and separately image the microstructures in different depths.

Furthermore, we measured the modulation transfer function (MTF) of the ballistic imaging systems with the object located object plane and moved to $\pm 600\,\mu$m along the light-propagation direction. The scattering medium used in this experiment was a suspension of 1.6-μm-diameter PS with OD of 6.The results are shown in Fig. 3. In this experiment, the imaging object was replaced by a United States Air Force test pattern (RT-MIL-TP2001, RealLight, Beijing, China). The location labeled as "0" is the object plane in focus.

From Fig. 3, we can see that the MTF curve of the DRBI system with the object at zero position has a slow descending tendency, while it falls rapidly for the conventional 4*f* ballistic imaging system. As shown in Fig. 3(a), the MTF curves of the DRBI system at $\pm 600\,\mu$m show a slow decline. Then both curves of the DRBI system at $\pm 600\,\mu$m are obviously away from which at zero location when the resolution test patterns are smaller than 28.5 line pairs/mm. For example, the contrast for 32 line pairs/mm (corresponding to an object size of 15.65 μm) at 0 location decreased rapidly from approximately 0.9 to 0.4 at $\pm 600\,\mu$m. In contrast, the MTF curves for the 4*f* ballistic imaging system with the test target at $\pm 600\,\mu$m decline without obvious deviation from the MTF curve at zero location as shown in Fig. 3(b). From the insets of Fig. 3, we can directly observe that the images at

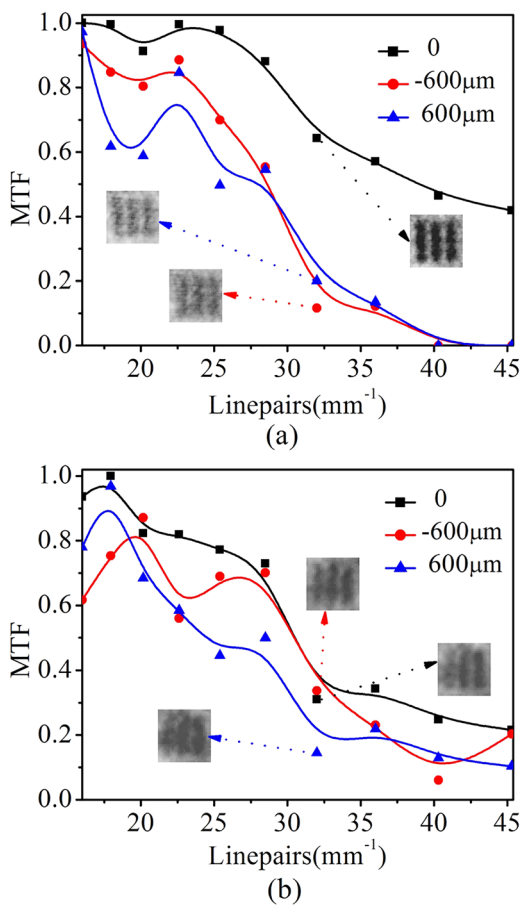

FIG. 3. (a) MTFs of the DRBI system; (b) MTFs of the 4*f* ballistic imaging system. The images of a test pattern of approximately 15.63-μm width at different locations are shown in the insets.

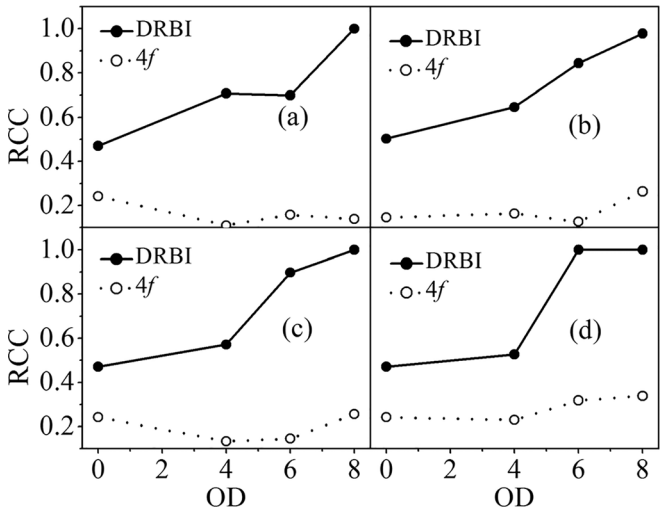

FIG. 4. Relatively contrast changes (RCCs) of the DRBI system (squares) and the conventional 4*f* ballistic imaging system (circles) at different ODs and scattering particle sizes: (a) 0.713 μm. (b) 1.6 μm. (c) 3.13 μm. (d) 4.46 μm.

± 600 μm blurred seriously compared with the clear image at zero location in the DRBI system, while the corresponding images have very few variations in the conventional 4*f* imaging system. These results confirm the depth-resolved capability of the DRBI system.

We further compared the depth-resolved imaging capability of the two imaging systems for different scattering environments, in which similar to measurements performed above, the contrast for 32 line pairs/mm in and 600-μm away from the object plane were measured as the criteria. The PS suspensions of sphere sizes of 0.71 μm, 1.60 μm, 3.13 μm, and 4.16 μm at different ODs of 0, 4, 6, and 8 were used. A relatively contrast change (RCC) was used to characterize the depth-resolved imaging capability, which was defined as $\mathrm{RCC} = |C_{\mathrm{in}} - C_{\mathrm{out}}|/C_{\mathrm{in}}$. Here, C_{in} and C_{out} are the imaging contrasts of object in and away from the object plane, respectively. The depth-resolved imaging capabilities are highest at $\mathrm{RCC} = 1$ and lowest at $\mathrm{RCC} = 0$.

It can be seen from Fig. 4(a) that the RCCs of the DRBI system are higher and increase with increasing the ODs, while the RCCs of the conventional 4*f* ballistic imaging system are lower and have slow variations at different ODs. The results show that comparing with the depth-resolved imaging capability of the conventional 4*f* imaging system, which of the DRBI system is higher and will increase with increasing the ODs. We infer the reason as follows: in the DBRI system, the subjects away from the object plane will form blurrier images and even form a weak background extremely. When the ODs of the scattering environments were increased, the residual scattered photons passing through the OKG will more enhance the degeneration of the subject visibility away from the object plane. Thus, under high scattering environments, the depth-resolved imaging capability of the DRBI system will increase with increasing the ODs. The similar results can be also seen for the 1.6-μm, 3.13-μm, and 4.46-μm PS suspensions as shown in Figs. 4(b)–4(d). Besides, from Figs. 4(a)–4(d) we can also see that the RCCs versus the ODs for the DRBI system increase more quickly with increasing the scattering particle size. This can be attributed to that the residual scattered photons passing through the OKG increase with increasing the scattering particle size.

CONCLUSION

In conclusion, we experimentally demonstrated depth-resolved imaging using a ballistic imaging system, in which a heterodyned femtosecond optical Kerr gate is introduced to extract useful imaging photons for detecting an object hidden in turbid media and a compound lens is proposed to ensure both the depth-resolved imaging capability and the long working distance. By taking advantage of its low DOF, two objects of about 15-μm widths hidden in a polystyrene-sphere suspension were imaged with 600-μm depth resolution. Moreover, we measured and compared the MTFs of the DRBI system and the conventional 4f ballistic imaging system in different scattering media. The results indicated that comparing with the depth-resolved imaging capability of the conventional 4*f* ballistic imaging system, which of the DRBI system is higher and will increase with increasing the ODs or scattering particle sizes of the scattering environments. This low-DOF ballistic imaging approach might be feasible to the research of the internal structure of a high-scattering fuel spray.

ACKNOWLEDGMENTS

The authors gratefully acknowledge the financial support for this work provided by the National Natural Science Foundation of China under Grant Nos. 61427816, 61235003, 61205129, and 61308036 and the Natural Science Basic Research Plan in Shaanxi Province of China (Program No. 2014JQ8363). This work was also supported by Collaborative Innovation Center of Suzhou Nano Science and Technology.

[1]K. M. Yoo and R. R. Alfano, Opt. Lett. **15**, 320 (1990).
[2]L. Wang, P. P. Ho, C. Liu, G. Zhang, and R. R. Alfano, Science **253**, 769 (1991).
[3]M. Paciaroni and M. Linne, Appl. Opt. **43**, 5100 (2004).
[4]M. A. Linne, M. Paciaroni, J. R. Gord, and T. R. Meyer, Appl. Opt. **44**, 6627 (2005).
[5]S. Idlahcen, L. Méès, C. Rozé, T. Girasole, and J. B. Blaisot, J. Opt. Soc. Am. A **26**, 1995 (2009).
[6]F. X. d'Abzac, M. Kervella, L. Hespel, and T. Dartigalongue, Opt. Express **20**, 9604 (2012).
[7]S. Xu, W. Tan, J. Si, P. Zhan, J. Tong, and X. Hou, Opt. Express **23**, 1800 (2015).
[8]P. Zhan, W. Tan, J. Si, S. Xu, J. Tong, and X. Hou, Appl. Phys. Lett. **104**, 211907 (2014).
[9]H. Purwar, S. Idlahcen, C. Rozé, D. Sedarsky, and J. B. Blaisot, Opt. Express **22**, 15778 (2014).
[10]F. Mathieu, M. A. Reddemann, J. Palmer, and R. Kneer, Opt. Express **22**, 7058 (2014).
[11]*Basic Photographic Materials and Processes*, edited by L. Stroebel (Boston: Focal Press, 1990).
[12]W. Tan, P. Zhan, J. Si, S. Xu, J. Tong, H. Xu, and X. Hou, Opt. Express **22**, 28100 (2014).
[13]M. E. Orczyk, M. Samoc, J. Swiatkiewicz, and P. N. Prasad, J. Chem. Phys. **98**, 2524 (1993).
[14]J. Tong, Y. Yang, J. Si, W. Tan, F. Chen, W. Yi, and X. Hou, Opt. Eng. **50**, 043607 (2011).